Monthly Notices of the ROYAL ASTRONOMICAL SOCIETY

MNRAS **460,** L94–L98 (2016) doi:10.1093/mnrasl/slw086
Advance Access publication 2016 April 29

Spiral-induced velocity and metallicity patterns in a cosmological zoom simulation of a Milky Way-sized galaxy

Robert J. J. Grand,[1,2]★ Volker Springel,[1,2] Daisuke Kawata,[3] Ivan Minchev,[4] Patricia Sánchez-Blázquez,[5,6] Facundo A. Gómez,[7] Federico Marinacci,[8] Rüdiger Pakmor[1] and David J. R. Campbell[9]

[1]*Heidelberger Institut für Theoretische Studien, Schloss-Wolfsbrunnenweg 35, D-69118 Heidelberg, Germany*
[2]*Zentrum für Astronomie der Universität Heidelberg, Astronomisches Recheninstitut, Mönchhofstr. 12-14, D-69120 Heidelberg, Germany*
[3]*Mullard Space Science Laboratory, University College London, Holmbury St Mary, Dorking, Surrey RH5 6NT, UK*
[4]*Leibniz-Institut für Astrophysik Potsdam (AIP), An der Sternwarte 16, D-14482 Potsdam, Germany*
[5]*Departamento de Física Teórica, Universidad Autónoma de Madrid, Cantoblanco E-28049, Spain*
[6]*Instituto de Astrofísica, Universidad Pontifica Católica de Chile, Av. Vicuña Mackenna 4860, Santiago, Chile*
[7]*Max-Planck-Institut für Astrophysik, Karl-Schwarzschild-Str. 1, D-85748 Garching, Germany*
[8]*Department of Physics, Kavli Institute for Astrophysics and Space Research, MIT, Cambridge, MA 02139, USA*
[9]*Department of Physics, Institute for Computational Cosmology, Durham University, South Road, Durham DH1 3LE, UK*

Accepted 2016 April 26. Received 2016 April 26; in original form 2016 April 4

ABSTRACT

We use a high-resolution cosmological zoom simulation of a Milky Way-sized halo to study the observable features in velocity and metallicity space associated with the dynamical influence of spiral arms. For the first time, we demonstrate that spiral arms, that form in a disc in a fully cosmological environment with realistic galaxy formation physics, drive large-scale systematic streaming motions. In particular, on the trailing edge of the spiral arms the peculiar galactocentric radial and azimuthal velocity field is directed radially outward and azimuthally backward, whereas it is radially inward and azimuthally forward on the leading edge. Owing to the negative radial metallicity gradient, this systematic motion drives, at a given radius, an azimuthal variation in the residual metallicity that is characterized by a metal-rich trailing edge and a metal-poor leading edge. We show that these signatures are theoretically observable in external galaxies with integral field unit instruments such as VLT/MUSE, and if detected, would provide evidence for large-scale systematic radial migration driven by spiral arms.

Key words: galaxies: evolution – galaxies: kinematics and dynamics – galaxies: spiral – galaxies: structure.

1 INTRODUCTION

Spiral arms are typical features of late-type disc galaxies, which make up roughly ∼70 per cent of the bright galaxies in the local volume. They are found not only in the distribution of cold gas and young, bright stars, but also in the old stellar populations (Rix & Zaritsky 1995), which indicate that they are a dynamical phenomenon. Most theoretical models in the last 50 yr have centred on variations of the classic density wave theory (Lin & Shu 1964) or swing amplification theory (Julian & Toomre 1966). In the former, the spiral density enhancement is regarded as a crest of stars that preserves its shape as it propagates around the disc, whereas in the latter it is described by a shearing overdensity that grows and decays around a preferred pitch angle (e.g. Baba, Saitoh & Wada 2013; Grand, Kawata & Cropper 2013; Michikoshi & Kokubo 2014). In the last decades, many observational attempts have been made to test these theories, using methods such as the Tremaine–Weinberg equations (Tremaine & Weinberg 1984) and the spatial distribution of star forming tracers (e.g. Foyle et al. 2010; Ferreras et al. 2012). However, despite decades of study, the nature of spiral arms remains an unsolved problem in contemporary astrophysics.

In recent years, numerical simulations have provided new insights into the formation and evolution of spiral arms. Crucially, *N*-body simulations commonly show transient spiral arms (Sellwood 2011), which form and disrupt on the order of a dynamical time. An important secular effect of transient spiral arms is their ability to change the angular momentum of individual star particles around the co-rotation radius, which over several dynamical times leads to significant radial mixing of star particles throughout the disc (Sellwood & Binney 2002). Grand, Kawata & Cropper (2012a) showed that transient spiral arms appear to wind-up

★E-mail: robert.grand@h-its.org

because of their co-rotation with disc particles at all radii, which can induce systematic motion of star particles along the leading and trailing edges of the spiral arms (Grand, Kawata & Cropper 2014; Kawata et al. 2014), in addition to changing the metal distribution in the disc (Grand, Kawata & Cropper 2015a).

The majority of simulations used for the study of spiral arms are set up in isolated, idealized initial conditions, such as pure exponential discs set up in equilibrium and in the absence of many important aspects of galaxy formation physics such as stellar accretion and gas inflows/outflows. While a major advantage of these simulations is the ability to control parameters and study individual effects, the lack of a realistic cosmological setting can limit their predictive power in the sense that the predicted relations between kinematics, metallicity, and age may be somewhat artificial, particularly over cosmological time-scales. In this Letter, we show for the first time systematic radial migration around the spiral arms in a high-resolution self-consistent cosmological simulation which includes a wide range of galaxy formation physics. This implies that the nature of spiral arms is similar to the transient, winding spiral density enhancements commonly seen in idealized *N*-body simulations. Furthermore, we demonstrate for the first time that the systematic motion drives clear patterns of azimuthal variation of the metallicity distribution. We demonstrate that the peculiar velocity field and metallicity distribution around the spiral arms can be detected with current integral field unit (IFU) instruments, such as VLT/MUSE (Bacon et al. 2010).

2 NUMERICAL SIMULATION

We focus on one high-resolution cosmological zoom simulation taken from the Auriga simulation suite (see Grand et al. 2016 and Grand et al., in preparation for a full description), performed with the state-of-the-art magnetohydrodynamical moving-mesh code AREPO (Springel 2010). The halo was initially selected from a parent dark matter only cosmological simulation of comoving periodic box size 100 Mpc, with the standard Λcold dark matter cosmology. The adopted cosmological parameters are $\Omega_{\rm m} = 0.307$, $\Omega_{\rm b} = 0.048$, $\Omega_\Lambda = 0.693$ and a Hubble constant of $H_0 = 100\,h\,{\rm km\,s^{-1}\,Mpc^{-1}}$, where $h = 0.6777$, taken from Planck Collaboration XVI (2014). At the end-point of this simulation, candidate haloes were selected within a narrow mass range interval around $10^{12}\,{\rm M}_\odot$ which are located at least 1.37 Mpc from any object more than half the mass of the candidate at $z = 0$, in order to select a sample of Milky Way size systems that are relatively isolated. At $z = 127$, the resolution of the dark matter particles of this halo is increased and gas added to create the initial conditions of the zoom, which is then evolved to present day. The typical mass of a high-resolution dark matter particle is $\sim 3 \times 10^5\,{\rm M}_\odot$, and the baryonic mass resolution is $\sim 4 \times 10^4\,{\rm M}_\odot$, with a maximum physical softening length equal to 369 pc (see Grand et al. 2016).

The simulation includes a comprehensive galaxy formation model (see Vogelsberger et al. 2013; Marinacci, Pakmor & Springel 2014; Grand et al. 2016, for more details), which reproduces many of the global properties representative of observed galaxy populations, such as the stellar-to-halo mass function, cosmic star formation rate density and galaxy morphologies. The simulation discussed in this study is Au 25 presented in Grand et al. (2016), which is a relatively isolated galaxy that displays clear two-armed spiral structure and is therefore an ideal choice to study the nature of spiral arms in cosmological simulations and their effects on disc chemo-dynamics.

3 RESULTS

Spiral structure is situated in the disc component of galaxies, and it follows that stars that spend much of their orbit in the disc mid-plane are dynamically responsive to such structures. We therefore focus our analysis on young stars (age <3 Gyr) that belong to the thin disc, which constitute about 27 per cent of the total stellar mass within a radius of 25 kpc. Note that if all star particles were to be considered, the observable features described in this Letter would be weaker, owing to contamination of bulge and halo stars. We focus on a single snapshot of galaxy Au 25 at a lookback time of 2.67 Gyr, which we choose because of its late time, quiescent environment, and well-formed spiral arms in order to demonstrate clearly the dynamical signatures related to spiral structure, which is the aim of this study. The nature of the spiral arms and their evolution will be studied in a forthcoming paper.

3.1 Velocity fields

In the following, we define the azimuthal peculiar velocity, V_ϕ, as the difference between the azimuthal velocity of a star particle and the mean rotation velocity at the particle radius, and define $V_\phi > 0$ as faster than mean rotation. The radial and vertical peculiar velocities, V_R and V_Z, are defined as the radial and vertical velocities, with $V_R > 0$ towards the galactic anticentre and $V_Z > 0$ towards the North Galactic Pole.

In the left-hand panel of Fig. 1, we show the face-on map of V_ϕ, with azimuthal overdensity contours of the mass distribution, given by $(\Sigma(R, \phi) - \Sigma(R))/\Sigma(R)$, overlaid in white contours. The spiral structure extends from about 5 to 15 kpc, and is accompanied by a well-defined spiral-shaped pattern in the azimuthal peculiar velocity field: stars rotate locally slower on the trailing side of the spiral arm, whereas they rotate locally faster on the leading side. The middle panel of Fig. 1 shows the face-on map of V_R. Similarly, this velocity field reveals a spiral-shaped pattern in which the spiral arm locus delineates the outward and inward streaming motions that are situated on the trailing and leading sides of the spirals, respectively. The right-hand panel of Fig. 1 shows the face-on map of V_Z, the fluctuations of which are of a lower amplitude in comparison to the planar velocity fields. We note that there may be indications of vertical modes in this galaxy (such as those shown in Gómez et al. 2016), which will be investigated in a forthcoming paper (Gomez et al., in preparation).

These patterns in the velocity fields are qualitatively similar to the systematic motions discussed in several recent studies of idealized simulations of isolated discs (e.g. Kawata et al. 2014; Grand et al. 2015b; Hunt et al. 2015) and in some observational work (e.g. Chemin, Renaud & Soubiran 2015). In the former studies, the systematic motions have been linked to transient, winding spiral density enhancements commonly seen in *N*-body simulations, in which star particles on the trailing or leading side of the spiral maintain their position with respect to the spiral peak, and are continuously torqued to larger or smaller guiding centre radii (Grand et al. 2012a, 2014; Grand, Kawata & Cropper 2012b).

3.2 Metal distribution

The torques applied to stars from spiral arms that generate the systematic streaming motions play a significant role in re-distributing individual stars around the disc, a process referred to as radial migration (Sellwood & Binney 2002; Minchev & Famaey 2010; Grand et al. 2012a). For a disc with a negative radial metallicity gradient,

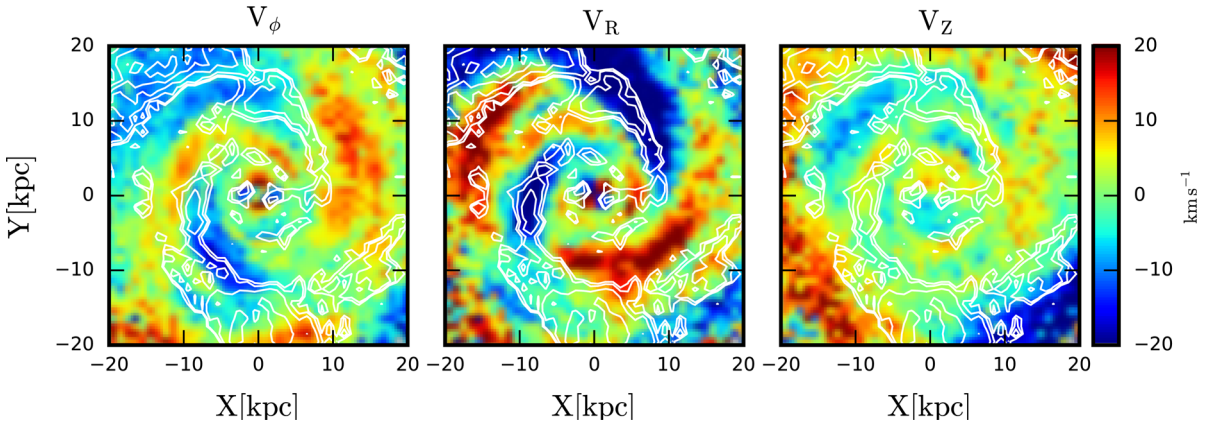

Figure 1. Face-on maps of the azimuthal (left), radial (middle), and vertical (right) peculiar velocity fields. Positive velocities are in the direction of rotation (azimuthal), the galactic anticentre (radial) and positive vertical heights (vertical). Overdensity contours of the mass distribution are indicated by the contours. The azimuthal peculiar velocity field is systematically slower (faster) on the trailing (leading) edge of the spiral, whereas the radial peculiar velocity points outward (inward) on the trailing (leading) edge. The amplitude of the fluctuations in the vertical peculiar velocity field are lower than the planar velocity fields, and show a less coherent pattern.

such as that of the Milky Way (e.g. Boeche et al. 2013; Anders et al. 2014; Bergemann et al. 2014), the radial re-distribution of stars can lead to changes in the metal distribution, in particular metal-rich (poor) stars from the inner (outer) regions are brought to the outer (inner) regions. Such a radial re-distribution of stars has been shown to broaden the metallicity distribution (Minchev, Chiappini & Martig 2013; Grand, Kawata & Cropper 2015a), and is required to explain the large scatter in the age–metallicity relation in the solar neighbourhood (Chiappini, Matteucci & Romano 2001; Haywood 2008; Casagrande et al. 2011). However, the observation of these trends is possible in the Milky Way only, for which star-by-star measurements are available.

A more directly observable signature of radial migration along spiral arms may come from azimuthal trends of metallicity at a given radius, in much the same spirit as the velocity trends are found in Fig. 1. To date, the only study of such a signature from a simulation perspective is that of Di Matteo et al. (2013), who studied the azimuthal variation of the metallicity distribution of old stars around a bar and found a pattern characteristic of radial migration around the bar co-rotation radius. A detailed study of the azimuthal variations of chemical abundances in APOGEE data, and their relation to Milky Way spiral structure, will be presented in Minchev et al., in preparation (see also Bovy et al. 2014).

In the top panel of Fig. 2, we show the face-on map of the azimuthal residual metallicity distribution, defined as $\delta[\mathrm{Fe/H}](R,\phi) = [\mathrm{Fe/H}](R,\phi) - \overline{[\mathrm{Fe/H}]}(R)$. It is clear that in the radial range of spiral structure, the metallicity pattern is characterized by an overdensity of metal-rich stars on the trailing side of the spiral arm, whereas an overdensity of metal-poor stars are found on the leading side of the spiral. These features are a consequence of the radial metallicity distribution, which has a radial gradient of -0.035 dex kpc^{-1} and metallicity dispersion of about 0.19 dex at a given radius. We note that the trend is even more clear in the bottom panel of Fig. 2, in which the radial metallicity distribution is artificially set 120 Myr earlier (about a dynamical time) with a fixed radial gradient of -0.08 dex kpc^{-1} and a radially constant metallicity dispersion of 0.05 dex. This confirms that the dynamics are consistent with large-scale radial migration along the spiral arms, and also that the signatures become more clear for steeper radial gradients and narrower metallicity dispersions, respectively. This is the first time that such a trend has been shown, and provides a further observational test for the radial migration driven by spiral arms.

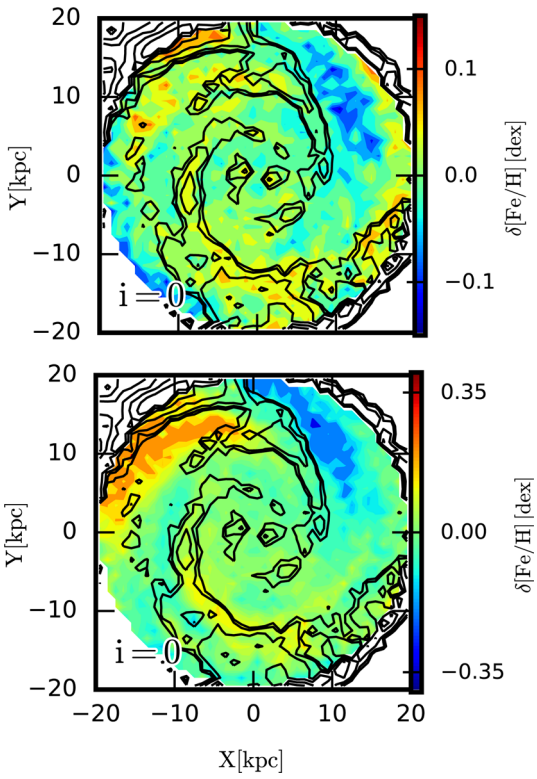

Figure 2. Face-on map (inclination, $i = 0$) of the azimuthal residual of the actual metallicity field (top panel) and that obtained for the case in which the metallicity field is artificially generated 120 Myr before the current time (bottom panel). Overdensity contours of the mass distribution are indicated by the contours. At many radii, there is an overdensity of metal-rich (-poor) star particles on the trailing (leading) side of the spiral arm.

3.3 Observing the line-of-sight signatures

The features of the peculiar velocity and residual metallicity fields shown above can be directly observed in external galaxies with IFU

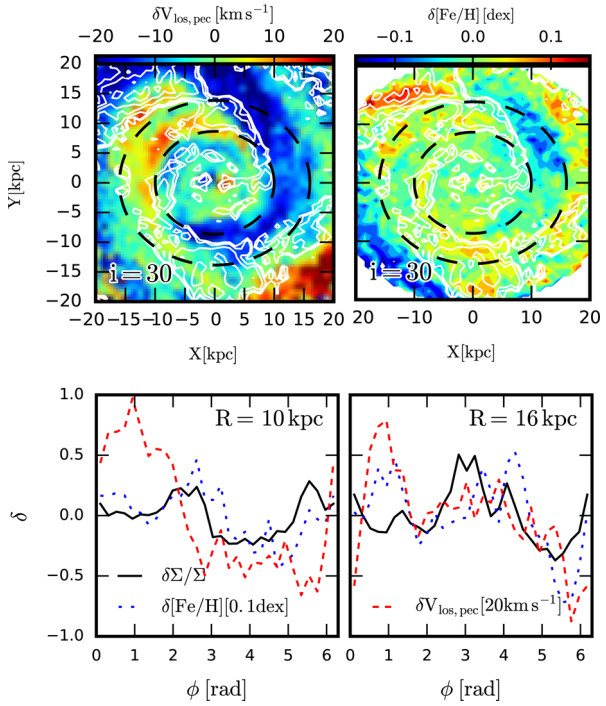

Figure 3. Top: the peculiar LOS velocity field (left) and residual metallicity (right) of the disc at an inclination of 30 deg. Positive LOS velocities are directed away from the observer. The dashed lines indicate galactocentric radii of 10 and 16 kpc. Bottom: the azimuthal profiles of the surface density (black solid), residual metallicity (blue dotted), and peculiar LOS velocity (red dashed) at radii of 10 (left) and 16 (right) kpc. $\phi = 0$ corresponds to $X = 0$ for $Y > 0$, and increases with counter-clockwise rotation in the disc plane.

instruments, such as VLT/MUSE. To demonstrate how the peculiar velocity field and metallicity distribution are mapped to the line-of-sight (LOS) velocity field,[1] $\delta V_{\rm los,pec}$, and LOS metallicity distribution, we set the disc to an inclination of 30 deg, which is enough inclined to observe planar peculiar velocities while maintaining a clear view of the spiral structure. The projected LOS peculiar velocity map and residual metallicity map are shown in the top panels of Fig. 3. For $X < 0$, positive V_ϕ is mapped to positive LOS velocities (away from the observer), and to negative LOS velocities (towards the observer) for $X > 0$. Positive V_R is mapped to positive LOS velocities for $Y > 0$, and negative LOS velocities for $Y < 0$.

To quantify the fluctuations in both fields, we show in the bottom panels of Fig. 3 the azimuthal profiles of the residuals of the mass surface density, metallicity, and LOS peculiar velocity fields at two different radii. We define $\phi = 0$ for $X = 0$ and $Y > 0$, which increases counter-clockwise in the disc plane. The patterns in the LOS peculiar velocity, $\delta V_{\rm los,pec}$, depend on the location of the spiral arms, because the direction of the LOS projection of the radial and azimuthal peculiar velocities flips around $Y = 0$ and $X = 0$, respectively. At $R = 10$ kpc, the spiral arm at $\phi \sim 5.5$ rad is located at $Y > 0$. Both the leading ($\phi < 5.5$ rad) and trailing side ($\phi > 5.5$ rad), have positive X and Y coordinates, where azimuthally fast (slow) and radially inward (outward) peculiar velocities on the leading (trailing) edge give rise to negative (positive) $\delta V_{\rm los,pec}$. Clockwise (decreasing ϕ) of this spiral arm, the $\delta V_{\rm los,pec}$ remains negative because the radially positive motion on the trailing edge of the next spiral ($\phi \sim 3.0$ rad) for $Y < 0$ is directed towards the observer. On the leading edge of this spiral arm ($\phi \sim 1.5$ rad), the large peculiar azimuthal velocity leads to a positive $\delta V_{\rm los,pec}$. A similar trend is present at $R = 16$ kpc, though there is a small additional peak at $\phi \sim 4.0$ owing to the phase shift in spiral arm position with respect to $R = 10$ kpc that causes negative peculiar azimuthal velocities on the trailing side of the spiral to contribute to positive $\delta V_{\rm los,pec}$ for $X > 0$ and $Y < 0$. The semi-amplitude of $\delta V_{\rm los,pec}$ is about 10–15 km s^{-1}. For the metallicity residuals, the semi-amplitude is ∼0.05 dex, which yields a total variation of ∼0.1 dex. The semi-amplitudes of the LOS peculiar velocity can be increased up to ∼20 km s^{-1} for inclinations up to ∼60 deg, however the spatial resolution is lower. The magnitudes of these fluctuations should be large enough to be detected with IFU observations of nearby late-type galaxies.

4 CONCLUSIONS

In this study, we have analysed signatures in the peculiar velocity and residual metallicity fields linked to the dynamical influence of spiral arms, in one of the high-resolution, fully cosmological zoom simulations from the Auriga suite (Grand et al. 2016). We have demonstrated that the peculiar azimuthal velocity is locally slower (faster) on the trailing (leading) edge of the spiral arm. Similarly, the peculiar radial velocity is directed radially outward (inward) on the trailing (leading) edge of the spiral arm, which in combination with the azimuthal velocity creates a systematic streaming motion along the spiral arm. This represents the first confirmation of systematic radial migration around spiral arms in a fully cosmological zoom simulation, which is in agreement with idealized *N*-body simulations of isolated discs that show transient, winding spiral arms.

In addition, we show for the first time that the radial migration caused by the spiral arms leads to azimuthal variations of the metallicity distribution: at a given radius, star particles that originated from interior regions of the disc are metal rich with respect to the azimuthal mean metallicity at that radius, because of the negative metallicity gradient commonly observed in disc galaxies. As indicated by the systematic streaming motions, the metal-rich particles are transported outward along the trailing edge of the spiral. Similarly, the metal-poor star particles that originate in the outer disc regions are transported radially inwards along the leading edge of the spiral. The result of these motions is a residual metallicity pattern in azimuth which is systematically more metal rich (poor) along the trailing (leading) edge of the spiral arm at many radii.

Finally, we have shown that the azimuthal variations of the peculiar LOS velocity and metallicity maps in a disc inclined at an angle of 30 deg are about 20–30 km s^{-1} and 0.1 dex, respectively. These variations can be detectable in nearby late-type spiral galaxies with IFU instruments such as VLT/MUSE.

We note that a systematic difference in azimuthal velocity across a density wave-like spiral arm has been suggested by Minchev & Quillen (2008) and Pasetto et al. (2015). However, these motions would depend on the location of the resonance points and are not expected to drive a metallicity variation around the spiral arm, because they are not associated with radial migration. The results of this Letter therefore represent a prediction of the dynamical influence of spiral arms on stars that differs qualitatively from that of density wave-like spirals (see also Monari, Famaey & Siebert 2016), and have the potential to test spiral arm formation mechanisms.

[1] We note that the contribution from the vertical peculiar velocity to the LOS velocity within this radial range is minor and does not affect the trends discussed in this Letter.

This Letter is an encouraging first step towards making new testable predictions of the systematic radial migration driven by spiral arms in fully cosmological simulations, which we have demonstrated are sufficiently advanced to study spiral arms. The exact values of the difference in the LOS velocities and residual azimuthal metallicity likely depend on the amplitude and pitch angle of spiral arms, the metallicity gradient, and the other properties of the thin disc. In future work, we will study a variety of spiral arm features using both cosmological and idealized simulations.

ACKNOWLEDGEMENTS

We thank the anonymous referee for a constructive report. RG and VS acknowledge support by the DFG Research Centre SFB-881 'The Milky Way System' through project A1. DJRC acknowledges STFC studentship ST/K501979/1. This work has also been supported by the European Research Council under ERC-StG grant EXAGAL-308037. Part of the simulations of this Letter used the SuperMUC system at the Leibniz Computing Centre, Garching, under the project PR85JE of the Gauss Centre for Supercomputing. This work used the DiRAC Data Centric system at Durham University, operated by the Institute for Computational Cosmology on behalf of the STFC DiRAC HPC Facility 'www.dirac.ac.uk'. This equipment was funded by BIS National E-infrastructure capital grant ST/K00042X/1, STFC capital grant ST/H008519/1, and STFC DiRAC Operations grant ST/K003267/1 and Durham University. DiRAC is part of the National E-Infrastructure.

REFERENCES

Anders F. et al., 2014, A&A, 564, A115
Baba J., Saitoh T. R., Wada K., 2013, ApJ, 763, 46
Bacon R. et al., 2010, in McLean I. S., Ramsay S. K., Takami H., eds, Proc. SPIE Conf. Ser. Vol. 7735, Ground-based and Airborne Instrumentation for Astronomy III. SPIE, Bellingham, p. 8
Bergemann M. et al., 2014, A&A, 565, A89
Boeche C. et al., 2013, A&A, 559, A59
Bovy J. et al., 2014, ApJ, 790, 127
Casagrande L., Schönrich R., Asplund M., Cassisi S., Ramírez I., Meléndez J., Bensby T., Feltzing S., 2011, A&A, 530, A138
Chemin L., Renaud F., Soubiran C., 2015, A&A, 578, A14
Chiappini C., Matteucci F., Romano D., 2001, ApJ, 554, 1044
Di Matteo P., Haywood M., Combes F., Semelin B., Snaith O. N., 2013, A&A, 553, A102
Ferreras I., Cropper M., Kawata D., Page M., Hoversten E. A., 2012, MNRAS, 424, 1636
Foyle K., Rix H.-W., Walter F., Leroy A. K., 2010, ApJ, 725, 534
Gómez F. A., White S. D. M., Marinacci F., Slater C. T., Grand R. J. J., Springel V., Pakmor R., 2016, MNRAS, 456, 2779
Grand R. J. J., Kawata D., Cropper M., 2012a, MNRAS, 421, 1529
Grand R. J. J., Kawata D., Cropper M., 2012b, MNRAS, 426, 167
Grand R. J. J., Kawata D., Cropper M., 2013, A&A, 553, A77
Grand R. J. J., Kawata D., Cropper M., 2014, MNRAS, 439, 623
Grand R. J. J., Kawata D., Cropper M., 2015a, MNRAS, 447, 4018
Grand R. J. J., Bovy J., Kawata D., Hunt J. A. S., Famaey B., Siebert A., Monari G., Cropper M., 2015b, MNRAS, 453, 1867
Grand R. J. J., Springel V., Gómez F. A., Marinacci F., Pakmor R., Campbell D. J. R., Jenkins A., 2016, MNRAS,
Haywood M., 2008, MNRAS, 388, 1175
Hunt J. A. S., Kawata D., Grand R. J. J., Minchev I., Pasetto S., Cropper M., 2015, MNRAS, 450, 2132
Julian W. H., Toomre A., 1966, ApJ, 146, 810
Kawata D., Hunt J. A. S., Grand R. J. J., Pasetto S., Cropper M., 2014, MNRAS, 443, 2757
Lin C. C., Shu F. H., 1964, ApJ, 140, 646
Marinacci F., Pakmor R., Springel V., 2014, MNRAS, 437, 1750
Michikoshi S., Kokubo E., 2014, ApJ, 787, 174
Minchev I., Famaey B., 2010, ApJ, 722, 112
Minchev I., Quillen A. C., 2008, MNRAS, 386, 1579
Minchev I., Chiappini C., Martig M., 2013, A&A, 558, A9
Monari G., Famaey B., Siebert A., 2016, MNRAS, 457, 2569
Pasetto S., Natale G., Kawata D., Chiosi C., Hunt J. A. S., 2015, preprint (arXiv:1512.05367)
Planck Collaboration XVI, 2014, A&A, 571, A16
Rix H.-W., Zaritsky D., 1995, ApJ, 447, 82
Sellwood J. A., 2011, MNRAS, 410, 1637
Sellwood J. A., Binney J. J., 2002, MNRAS, 336, 785
Springel V., 2010, MNRAS, 401, 791
Tremaine S., Weinberg M. D., 1984, ApJ, 282, L5
Vogelsberger M., Genel S., Sijacki D., Torrey P., Springel V., Hernquist L., 2013, MNRAS, 436, 3031

This paper has been typeset from a TEX/LATEX file prepared by the author.